Performance of Differential Chirp Spread Spectrum in Underwater Acoustic Channel

Marwane Rezzouki, Guillaume Ferré

▶ **To cite this version:**

Marwane Rezzouki, Guillaume Ferré. Performance of Differential Chirp Spread Spectrum in Underwater Acoustic Channel. 14th Latin American Symposium on Circuits and Systems (LASCAS 2023), Invited in WAFE session, Feb 2023, Quito, Ecuador. hal-04053983

HAL Id: hal-04053983
https://hal.science/hal-04053983

Submitted on 28 Nov 2023

HAL is a multi-disciplinary open access archive for the deposit and dissemination of scientific research documents, whether they are published or not. The documents may come from teaching and research institutions in France or abroad, or from public or private research centers.

L'archive ouverte pluridisciplinaire **HAL**, est destinée au dépôt et à la diffusion de documents scientifiques de niveau recherche, publiés ou non, émanant des établissements d'enseignement et de recherche français ou étrangers, des laboratoires publics ou privés.

Performance of Differential Chirp Spread Spectrum in Underwater Acoustic Channel

Marwane REZZOUKI and Guillaume FERRÉ
Univ. Bordeaux, CNRS, Bordeaux INP, IMS, UMR 5218, F-33400, Talence, France
marwane.rezzouki@ims-bordeaux.fr, guillaume.ferre@ims-bordeaux.fr

***Abstract*—In recent years, connecting fishing nets underwater has received much interest in carrying out fishing activities efficiently and protecting the ocean from pollution, especially from ghost fishing. In this paper, we propose an implementation of a system based on the differential chirp spread spectrum (DCSS) technique to connect fishing nets underwater while preserving the biotope from acoustic pollution. This technique is based on differential encoding, making it more robust to Doppler shift. Besides, it exploits the orthogonality of chirps to deal with inter-symbol interference and improve spectral efficiency. Furthermore, an estimation of the channel and equalization processes are used to eliminate the multipath effect which is very present in underwater acoustic (UWA) channels. The performance of our system is evaluated in terms of bit error rate (BER) in a lake trial.**

***Index Terms*—Connected fishing nets, differential chirp spread spectrum, DCSS system, low acoustic noise.**

I. INTRODUCTION

The fishery sector plays a central role in food security in many countries. According to the food and agriculture organization, fish consumption has doubled since the 1960s and as of 2019 capture production accounted for 92.5 million tonnes [1]. This huge production is a result of multiple factors as population growth and the need for resources rich in proteins and vitamins.

The introduction of underwater acoustic communication over the last decades enables diverse applications in civil and military sectors such as connecting autonomous underwater vehicles (AUV), deploying underwater sensor networks (USNs), and navigation [2]. In the fishery area, communication would help fishers to conduct efficiently their job. Indeed, by ensuring data link communication the angler could track the areas of fishing by measuring parameters such as salinity and temperature. Moreover, communication could prevent fishers in case of danger by detecting swells and alerting them. However, using a large network in the ocean based on acoustic waves with high power will pollute acoustically the environment and participate in the migration of species as mentioned in [3]. In this context, we focused on a particular technique of communication which is based on linear frequency modulation (chirps) to communicate in underwater acoustic (UWA) channels. The proposed technique is called differential chirp spread spectrum (DCSS) and it offers the ability to deploy a less disruptive network for marine animals. By sacrificing spectral efficiency, it will be possible to communicate at low values of signal-to-noise ratio (SNR). Therefore, the transmitted signals in the medium will be almost inaudible for marine animals.

Due to the physical properties of underwater acoustic channels, the transmitted signal may undergo a major degradation. The main characteristics of an UWA channel are multipath propagation because of the reflection of the acoustic wave on the surface and seafloor, severe Doppler shift, and spread, and finally high time variability.

In order to face the aforementioned characteristics of the channel, [4] added to the conventional chirp spread spectrum (CSS) technique processes to make the communication robust such as the differential encoding process to reduce the Doppler shift effect. Besides, channel estimation and equalization are used to eliminate the multipath effect. In this paper, we focus on the implementation of the DCSS system presented in [4] and its performance in a lake trial. The rest of this paper is organized as follows, in section II we introduce the architecture of DCSS and explain each part of it. In section III we introduce the hardware used to test the DCSS system. Section IV is dedicated to measurement results in lake trial and discussion. Finally, a conclusion is provided.

II. DIFFERENTIAL CHIRP SPREAD SPECTRUM

A. DCSS technique

At the transmitter, the binary frame is divided into several sub-sequences from the most significant bit, each of the length SF bits to constitute a symbol. Then, the summation of two consecutive symbols is performed to generate the symbols to transmit as mentioned in equation (1).

$$S_p = m_p + S_{p-1} \mod M \ , \ p \geq 1 \tag{1}$$

where $m_p \in [\![0, M-1]\!]$ are the symbols obtained from the binary information, $M = 2^{SF}$ is the possible number of constellations, SF is the spreading factor and S_0 is fixed at 0 to initiate the process. The association of the symbol S_p to a chirp signal defined at time symbol T and within a bandwidth B is done through a temporal cyclic shift to the raw chirp $x_{ref}(n)$ sampled at $T_s = \frac{1}{B}$.

$$x_{ref}(n) = e^{j2\pi(\frac{1}{2M}n^2 - \frac{1}{2}n)} \ , \ n \in [\![0, M-1]\!] \tag{2}$$

Consequently, the modulated chirp discrete phase of the p^{th} symbol to transmit at time pT can be expressed as:

$$\phi_p(n) = \begin{cases} 2\pi \left[\frac{1}{2M}n^2 + (\frac{S_p}{M} - \frac{1}{2})n\right] & \text{for } n \in [\![0, M - S_p - 1]\!] \\ 2\pi \left[\frac{1}{2M}n^2 + (\frac{S_p}{M} - \frac{3}{2})n\right] & \text{for } n \in [\![M - S_p, M-1]\!] \end{cases}$$

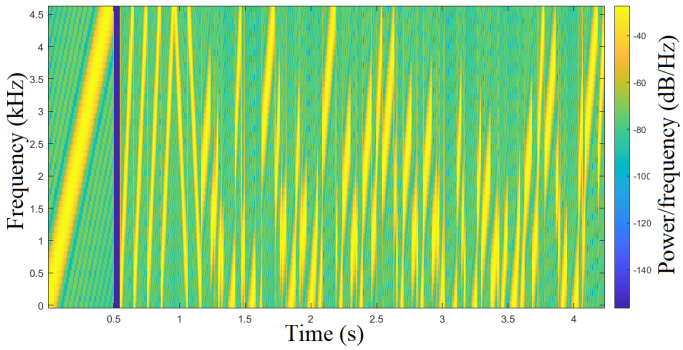

Fig. 1: Spectrogram of the transmitted signal in baseband

At the receiver, the transmitted signal is transformed by the impulse response of the UWA channel, and an additive white Gaussian noise is introduced to the signal. However, to understand the demodulation process, we consider only one path signal and we suppose that the received has perfect time and frequency synchronization. Thus, the expression of the discrete received signal at sampling time T_s is:

$$y(n) = \sum_{k=1}^{N_s} e^{j\phi_p(nTs-(k-1)T)} \mathbb{1}_{[(k-1)T,kT]}(n) \tag{3}$$

with N_s is the number of transmitted symbols and $\mathbb{1}_x(n)$ is the indicator function. The first step in demodulation consists in multiplying each symbol period of the received signal by the conjugate of the raw chirp $x_{ref}(n)$. Then, perform the fast Fourier transform (FFT) at every symbol time. Thus, the obtained FFT for each the p^{th} symbol can be expressed as follows:

$$Y_p[k] = \frac{1}{\sqrt{M}} \sum_{n=0}^{M-1} y_p(nT_s)\overline{x_{ref}(n)} e^{-j2\pi \frac{nk}{M}} \tag{4}$$

where $\overline{f(n)}$ is the conjugate of the function $f(n)$ $y_p(nT_s) = y(nT_s + (p-1)T)$ is the complex envelope of the p^{th} transmitted symbol.

Consequently, in a non-coherent receiver, a symbol $\tilde{S}_p$ is obtained by:

$$\tilde{S}_p = \underset{k\in[\![0,M-1]\!]}{\operatorname{argmax}} \left(|Y_p(k)|\right) \tag{5}$$

Finally, the original symbol $\tilde{m_p}$ can be obtained from the estimated symbol $\tilde{S}_p$ through differentiation using the following equation:

$$\tilde{m_p} = \tilde{S}_p - \tilde{S}_{p-1} \mod M \ , \ p \geq 1 \tag{6}$$

The main advantage of using differential encoding is to eliminate the constant frequency amount that could occur because of the Doppler effect or oscillators through differentiation in the frequency domain.

B. Transmitted signal

Fig. 1 illustrates the spectrogram of the transmitted frame. The signal is composed of a long chirp used to estimate the Doppler scale, a silence time greater than the delay spread of the channel, and a set of raw up chirps ($x_{ref}(n)$) followed by down chirps ($\overline{x_{ref}(n)}$) used for synchronization and channel estimation. The payload is generated using different spreading factors (5 and 6). Every two consecutive symbols have a different spreading factor to deal with the inter-symbol interference problem by exploiting the orthogonality of the chirps. Furthermore, it improves spectral efficiency because no silence time or cyclic prefix is needed.

C. Received signal

The proposed receiver is composed of several processes organized as follows:

1) Detection: Initially, the recorded signal is sub-sampled at time Ts and divided into several blocs, each of length M points that correspond to a symbol time. Then, each bloc is multiplied by the conjugate of the raw chirp $x_{ref}(nT_s)$, followed by an FFT operation. Finally, the argmax of the first peak of the FFT will coarsely indicate the first chirp in the preamble.

2) Doppler Estimation: The estimation of the Doppler scale consists of calculating the rate of received chirps. More precisely, a part of the long chirp in the preamble is used in the Fractional Fourier Transform (Frft) domain to estimate the new rate. According to [5], the optimal order of Frft corresponds to the rate of the chirp. Using the formula of the new rate and the expression of order, the Doppler scale can be simplified to:

$$\tilde{\Delta} = \sqrt{\frac{-cot(p_{opt}\frac{\pi}{2})}{\frac{B}{T_c}NT_s^2}} - 1 \tag{7}$$

where N is number of samples, T_c is the chirp duration, and p_{opt} is the optimal order.

3) Doppler Compensation: The compensation is made by re-sampling the recorded signal at $\frac{Ts}{1+\tilde{\Delta}}$ using a linear interpolation technique as mentioned in [6].

4) Synchronization: In this process, the raw up and down chirps in the preamble are used to estimate and compensate the amounts of desynchronization in both time and frequency domains [7].

Coarse synchronization: This part consists in multiplying each chirp by its conjugate and calculating the argmax of the FFT as mentioned in equation (5). As raw chirp is expected to be at zero, then the obtained values are the results of the desynchronization amounts. Therefore, combining the argmax of up chirps with argmax of down chirps leads to the expression of frequency and temporal synchronization.

Fine synchronization: At this point the received signal is resampled at rythm $\frac{1}{2B}$ and only up chirps are used to estimate the fraction part of desynchronization. The fractional part of carrier frequency offset is obtained by de-chirping the signal and calculating the phase. Whereas, the time amount is obtained as an average of argmax of FFT.

5) Channel Estimation: The channel estimation algorithm used is proposed in [8]. It is based on the received up chirps of the preamble and the raw up chirps in the preamble. Indeed, the raw chirp $x_{ref}(n)$, $n \in [\![0, M-1]\!]$ is used to constitute the circulant matrix $x_c(M, M)$ and the received chirps are used to

calculate the average vector $y_{Avg}(1, M)$. Thus, the temporal estimation of the channel $\hat{h}$ can be expressed as:

$$\hat{h} = \frac{x_c^H y_{Avg}}{x_c^H x_c} \tag{8}$$

6) Channel Equalization: The payload is rectified in the frequency domain using the minimum means square error (MMSE) equalizer [9]. Firstly, the signal is divided into several blocs, each of length M depending on SF used to generate symbols. Then the FFT is applied, followed by the multiplication of MMSE function transfer to each bloc. After that, inverse Fast Fourier transform (IFFT) is performed on each bloc. Finally, the estimation of symbols is carried out by applying the following operations of dechirping, calculating the argmax of FFT, and differentiation decoding as mentioned in part II-A.

III. Hardware used to test DCSS communication

To conduct experiments in UWA channels, we developed the system shown in Fig. 2. This system is divided into two parts:

- A transmitter composed of a signal generator, a power amplifier, and a transducer.
- A receiver composed of a hydrophone, a voltage pre-amplifier, and a data acquisition board.

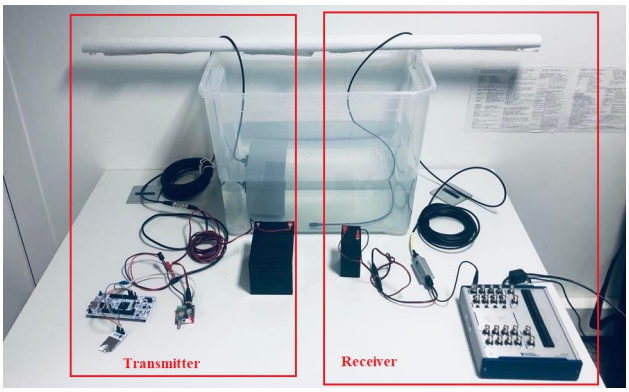

Fig. 2: Hardware of DCSS system

The signal generator is based on STM32F746 microcontroller that generates analog signal from stored sampled frame (at a sampling frequency of 100 kHz) as wave files in the micro SD. To drive the transducer BII-7506 we used PAM-8610 module that's amplify 1 V_{rms} output of the board into 15 V_{rms}. Thus, considering the transmitting voltage response of the transducer 157.6 dB 1 $\mu Pa/V$ @1m, the acoustic power of the transmitter is 181.1 dB re 1 μPa @1m. After crossing the channel, the signal is received by means of the hydrophone AS-1 (-208 dBV re 1 μPa). Then, the signal is amplified with a gain of 50 dB using an Low-noise broadband hydrophone amplifier PA-4. Finally, the signal is recorded using USB-6364 National instrument board connected to a laptop. The sampling frequency is programmable and limited to 500 kHz and the resolution of samples is 16 bits.

Fig. 3: Setup of the experiment

IV. Experiment results and discussion

A. Setup of experiments

The experiments are conducted in Bordeaux "Bassin a Flot" lake (see Fig. 3) at different ranges. The maximum distance between the transmitter and the receiver was 140 m, and it is chosen after establishing an acoustic link budget adapted to a lake environment and the characterization of the hardware in terms of the power of the transmitter and the sensitivity of the receiver. In addition, The depth of the lake was about 16 m, and both the transmitter and the receiver were fixed at a depth of 4 m. The main parameters used to generate the signal are listed in the table below.

TABLE I: Parameters of the transmitted signal

Parameter	Value
Carrier frequency	18 kHz
Sampling frequency	100 kHz
Bandwidth	2.5 kHz and 5 kHz
Preamble: Long chirp duration	1 s
Preamble: Number of up chirps	8
Preamble: Number of down chirps	2
payload: Double SF	5/6 and 6/7
Number of symbols	30

B. Impulse response of the channel

The estimation of the underwater acoustic channel is made using a set of hyperbolic frequency modulation (HFM) signals defined within a bandwidth of 5 kHz at a carrier frequency of 18 kHz, using a spreading factor of 9 and a time length of 120 ms. This technique is proposed in [10] and it consists in applying cross-correlation between the raw chirp and the received signal to obtain the variability of the channel and the power delay profile. As depicted in Fig. 4 the channel has three paths that vary slightly over time. As the most significant paths are located in an interval of time no longer than 4 ms, we can consider that the channel is sparse and its delay spread is less than the used symbol duration, which respects the condition of frequency selectivity of the channel.

C. Result of communication

The performance of the DCSS system is presented as bit error rate (BER) for different payload configurations at different ranges. The breakdown of each configuration is presented in Table II. As we can see the communication works perfectly when the distance between the transmitter and receiver was respectively 20 m and 60 m. However, at

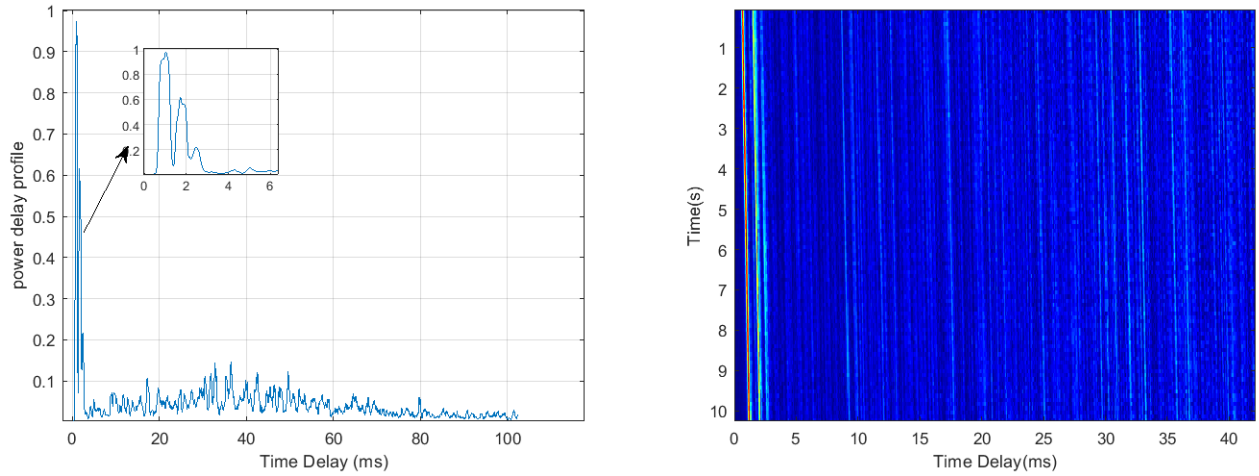

(a) Power delay profile

(b) The variability of the magnitude channel impulse response

Fig. 4: Underwater channel characteristics

TABLE II: Bit error rate

Range	Spreading factor		Bandwidth	Bitrate	BER
	Preamble	Payload			
20 m	6	5 and 6	5 kHz	572 bps	0
	6	5 and 6	2.5 kHz	286 bps	0
	7	6 and 7	5 kHz	338 bps	0
	7	6 and 7	2.5 kHz	169 bps	0
60 m	6	5 and 6	5 kHz	572 bps	0
	6	5 and 6	2.5 kHz	286 bps	0
	7	6 and 7	5 kHz	338 bps	0
	7	6 and 7	2.5 kHz	169 bps	$2.56\ 10^{-2}$
140 m	6	5 and 6	5 kHz	572 bps	$4.16\ 10^{-2}$
	6	5 and 6	2.5 kHz	286 bps	$3.33\ 10^{-2}$
	7	6 and 7	5 kHz	338 bps	$1.17\ 10^{-1}$
	7	6 and 7	2.5 kHz	169 bps	$9.87\ 10^{-2}$

a distance of 140 m, the obtained values of BER are low because the estimated channel presents a high level of noise. Consequently, the frequency equalization and demodulation processes are strongly impacted. Therefore, it is possible to enhance the result of this experiment through high acoustic power or a hydrophone with good receiving sensitivity.

V. Conclusion

In this work, we present the implementation of the DCSS system and its performance in a lake trial. The proposed DCSS receiver faces the severe characteristics of the UWA channel due to Doppler estimation and compensation in the fractional Fourier transform domain. Besides, channel estimation and MMSE equalization reduce significantly the multipath effect that could occur in such channels. These processes have low complexity and can be implemented in the FPGA board to ensure real-time communication. The experiments are conducted using a limited power amplifier. Driving the transducer with a better amplifier or having a hydrophone with a good receiving sensitivity would make long-range communication possible. Finally, the DCSS technique offers a good data link in the ocean environment because of its ability to demodulate the signal at low values of SNR which would preserve the biotop from acoustic noise. Further experiments will be carried out in diverse environments using different configurations to perform the DCSS system.

References

[1] "Fao. 2021. fao yearbook. fishery and aquaculture statistics 2019/fao annuaire. statistiques des pêches et de l'aquaculture 2019/fao anuario. estadísticas de pesca y acuicultura 2019. rome/roma." [Online]. Available: https://doi.org/10.4060/cb7874t

[2] N. J. Rowan, "The role of digital technologies in supporting and improving fishery and aquaculture across the supply chain – quo vadis?" *Aquaculture and Fisheries*, 2022. [Online]. Available: https://www.sciencedirect.com/science/article/pii/S2468550X22001010

[3] A. N. Rice, J. T. Tielens, B. J. Estabrook, C. A. Muirhead, A. Rahaman, M. Guerra, and C. W. Clark, "Variation of ocean acoustic environments along the western north atlantic coast: A case study in context of the right whale migration route," *Ecological Informatics*, vol. 21, pp. 89–99, 2014, ecological Acoustics. [Online]. Available: https://www.sciencedirect.com/science/article/pii/S1574954114000065

[4] M. Rezzouki, M. A. B. Temim, and G. Ferré, "Differential chirp spread spectrum to perform acoustic long range underwater localization and communication," in *OCEANS 2021: San Diego – Porto*, 2021, pp. 1–9.

[5] Y. Zhao, H. Yu, G. Wei, F. Ji, and F. Chen, "Parameter estimation of wideband underwater acoustic multipath channels based on fractional fourier transform," *IEEE Transactions on Signal Processing*, vol. 64, no. 20, pp. 5396–5408, 2016.

[6] C. Li, X. Shen, Z. Jiang, and X. Wang, "Mobile underwater acoustic communication based on passive time reversal," in *2017 IEEE International Conference on Signal Processing, Communications and Computing (ICSPCC)*, 2017, pp. 1–5.

[7] M. A. Ben Temim, G. Ferré, and R. Tajan, "A novel approach to enhance the robustness of lora-like phy layer to synchronization errors," in *GLOBECOM 2020 - 2020 IEEE Global Communications Conference*, 2020, pp. 1–6.

[8] I. B. F. de Almeida, M. Chafii, A. Nimr, and G. Fettweis, "Alternative chirp spread spectrum techniques for lpwans," *IEEE Transactions on Green Communications and Networking*, vol. 5, no. 4, pp. 1846–1855, dec 2021. [Online]. Available: https://doi.org/10.11092Ftgcn.2021.3085477

[9] K. Huang, R. Tao, and Y. Wang, "Study of frequency domain equalization for chirp spread spectrum systems," in *2010 IEEE International Conference on Wireless Communications, Networking and Information Security*, 2010, pp. 132–136.

[10] J. Schmidt, I. Kochańska, and A. Schmidt, "Measurement of impulse response of shallow water communication channel by correlation method," *HYDROACOUSTICS*, vol. 20, pp. 149–158, 2017.